RAYLEIGH-TAYLOR INSTABILITY OF A THIN LAYER

M. Fermigier, L. Limat, E. Wesfreid, P. Boudinet, C. Ghidaglia and C. Quilliet

Laboratoire de Physique et de Mécanique des Milieux Hétérogènes
Ecole Supérieure de Physique et de Chimie Industrielles
10 rue Vauquelin, 75231 Paris CEDEX 05, France

INTRODUCTION

In this communication, we report some recent results[1,2] obtained in the study of the Rayleigh-Taylor instability of a thin layer. This interfacial instability exhibits interesting "growth and form" effects, in which the non-linearities play an essential role: formation of two-dimensional patterns of different symmetries, transition between patterns (sometimes involving front propagation phenomena), secondary instabilities...

The Rayleigh-Taylor instability[3-5] is a gravitational instability occuring when there is an adverse density stratification in a fluid, for instance at the interface separating two fluids of different densities, the upper fluid being heavier than the lower one. Most of the available studies of its non-linear development deal with the case of thick layers, that is very important for practical applications: rising of magmas in geophysics[4], or laser implosion of fusion targets[5] for instance. Very few studies, based essentially on numerical simulations[6,7], have investigated the case in which one of the layers is very thin, its thickness e being in particular small compared to the capillar length $l_c=\sqrt{\rho g/\gamma}$ (as usual, $\rho=\rho_{up} - \rho_{down}$ designates the density difference, g the gravity and γ the surface tension). This case is also of practical importance, for instance in the genesis of two-phase flow in situations of film boiling[8,9].

EXPERIMENT - GENERAL OBSERVATIONS

In our experiment, a drop of silicone oil (viscosity η=1000 cP, density ρ=0.97 g/cm^3, surface tension γ=21 dynes/cm) is firstly spread by gravity on an horizontal glass plate yielding a viscous pancake, approximately 30 cm in diameter and a fraction of millimeter thick. Secondly, the instability is started by quickly inverting the plate. The development of the instability is then monitored by video recording or by photographs taken at fixed intervals. Figure (1) is a typical example obtained after 600 s. The deformation of the interface is revealed by means of a dye previously mixed with the oil. The thicker parts appear as dark spots on the picture. As can be seen on this figure, different patterns are obtained: axisymmetric patterns (concentric rings), axisymmetric patterns whose rings break into peaks (often with a sixfold symmetry), hexagonal patterns and finally, lines which we sometimes call "rolls", in analogy with the rolls observed in convective instabilities.

These patterns are in fact transient structures growing from initial perturbations of the interface. For instance the axisymmetric structures generally grow from the initial dimple created by specks of dusts on the interface. In a similar way, the "rolls" are initiated by the thickness gradient at the boundaries of the pancake. The evolution of the pattern seems then to involve three processes: (i) local growth of the amplitude (ii) spreading by an increase of their

Growth and Form, Edited by M. Ben Amar *et al.*
Plenum Press, New York, 1991

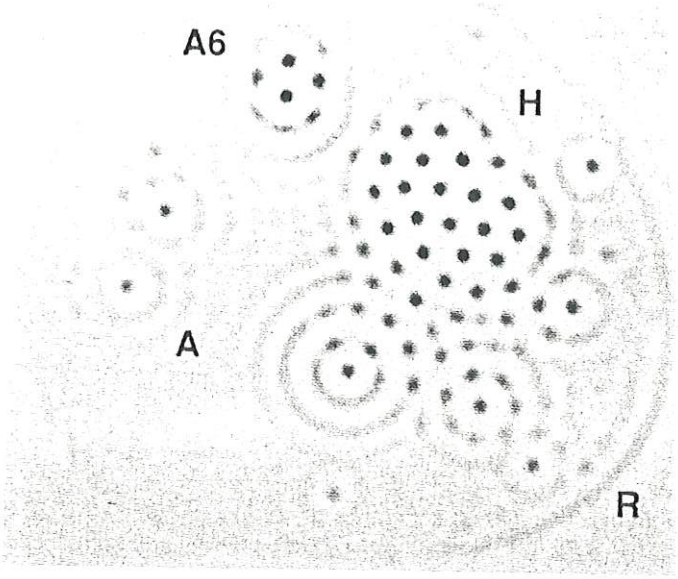

Fig. 1. Typical structures occuring in the instability. Thicker parts of the fluid appear as dark spots. (A) axisymmetric structures, (A6) axisymmetric structures developing a sixfold symmetry, (H) hexagonal pattern, (R) "rolls" or "lines" structures.

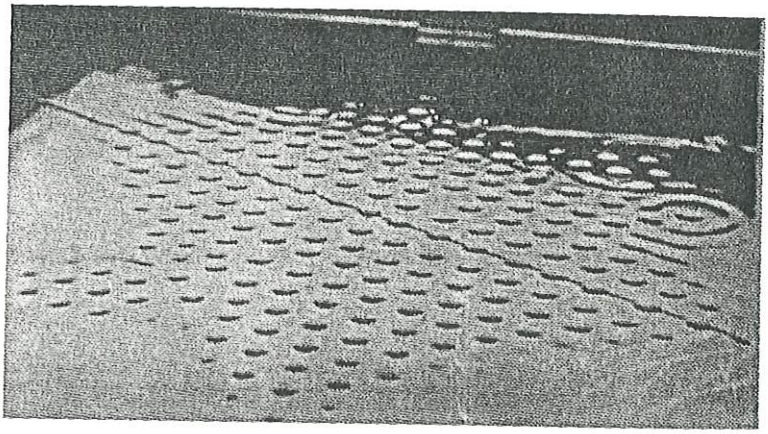

Fig. 2. Perspective view of the experiment seen from above, through the glass plate: a more or less regular hexagonal lattice of pendant drops connected by a very thin film is left below the plate in the final stage of the experiment.

spatial extent (iii) transition towards the hexagonal symmetry. After a complicated history, one finally gets a more or less ordered hexagonal system of pendant drops (see figure 2). In the latest stage, depending on the initial thickness, these drops can exhibit secondary instabilities: drop falling, drop coalescence, falling after coalescence...

EVOLUTION EQUATION - LINEAR GROWTH

The evolution equation governing the thickness variation $\zeta(\mathbf{r},t)=e(\mathbf{r},t) - e_0$ can be derived rather easily in the lubrication approximation, the slope of the interface of order e_o/l_c being assumed to be small[1,6,7] (This approximation neglects inertial effects and assumes that the horizontal dependance of the velocity field is negligible compared to the vertical one):

$$\frac{\partial \zeta}{\partial t} + \frac{1}{3\eta}\nabla.[(e_o+\zeta)^3\nabla(\rho g\zeta+\gamma\Delta\zeta)] = 0 \qquad (1)$$

This is the mass conservation equation, in which the mass flux is proportional to the pressure gradient $\nabla P=\nabla[\rho g\zeta+\gamma\nabla^2\zeta]$. This pressure gradient involves an hydrostatic contribution $\rho g\zeta$ associated to the destabilizing gravity, and a capillary one dependant upon the curvature of the interface. The fact that the "mobility" of the fluid is proportional to the cube of the thickness $e^3=(e_o+\zeta)^3$, results from the structure of the flow that reduces to a half-Poiseuille one. After linearizing this equation, one gets the dispersion relationship of Fourier modes $\exp[iqx+\sigma t]$:

$$\sigma = \frac{e_o^3}{3\eta}[\rho g q^2 - \gamma q^4] \qquad (2)$$

The variation of σ versus q is suggested below:

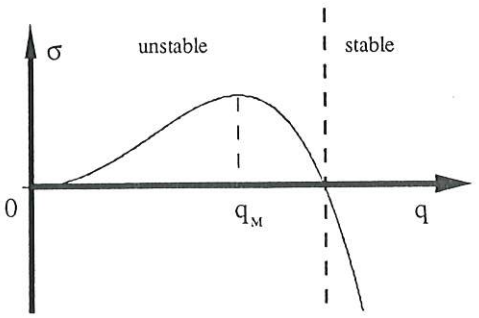

A large band of Fourier modes are unstable, the maximum growth rate being obtained for a wave number $q_M = \sqrt{\rho g/2\gamma}$. The associated wave-length $\lambda_M = 2\pi\sqrt{2}\, l_c \approx 13.2$ mm is consistent with that observed in our experiments (of order 12.5 mm for the most regular patterns).

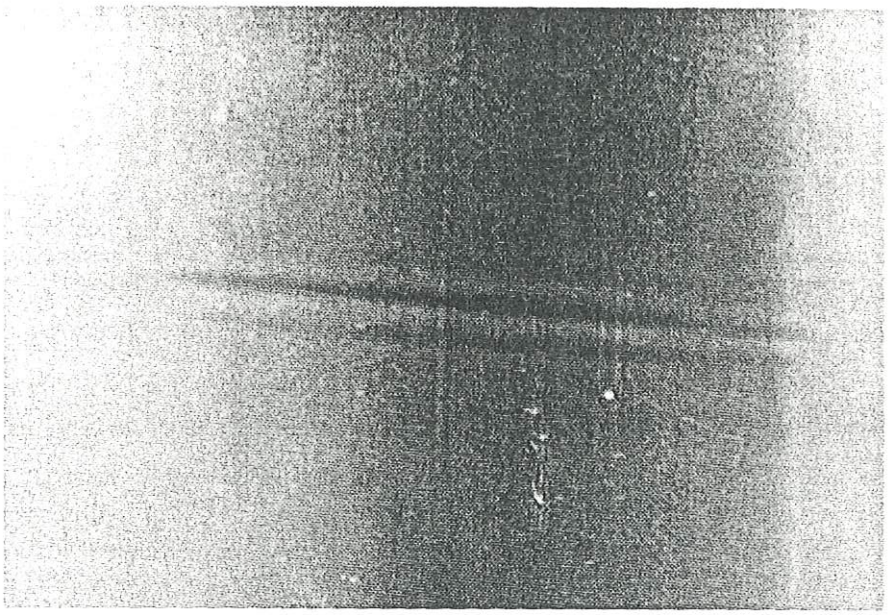

Fig. 3. Instability initiated by a single wire stretched through the fluid layer.

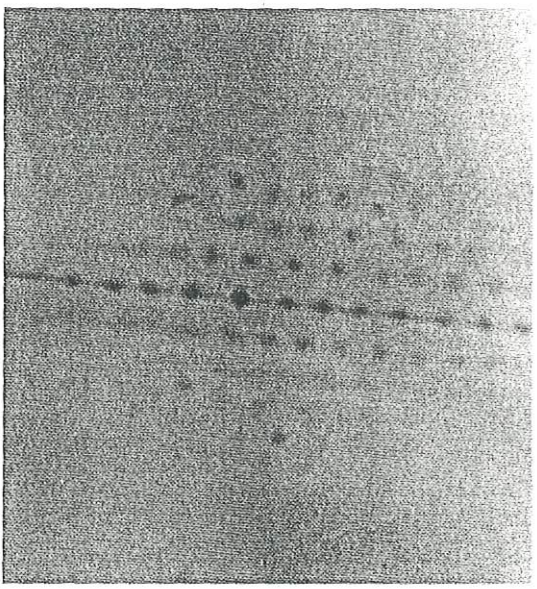

Fig. 4 Transition of the roll system of fig. 3 towards an hexagonal symmetry.

TRANSITION ROLLS-HEXAGONS

We have investigated the time evolution of the patterns, starting from well defined, controled initial conditions. In a first experiment, a thin metal wire is stretched across the oil layer after the spreading is completed. The wire has a diameter slightly larger than the oil thickness, and induces an initial perturbation which decays exponentially away from the wire, with a characteristic length equal to l_c. Once the glass plate is inverted, "rolls" developed parallel to the wire (see fig.3). These structures do not remain one-dimensional: after a while, the lines break in peaks of an hexagonal pattern (fig. 4).

This tendency of our system to form an hexagonal pattern can be roughly explained[1] by expanding eq. (1) over the Fourier modes. After some calculations, the evolution equation of the amplitude $A_q(t)$ of a mode q is given by:

$$\frac{dA_q}{dt} = (2q^2-q^4)\,A_q + 3 \sum_{q_a,q_b} (q_a.q)(2-q_a^2)A_{qa}A_{qb}\delta(q-q_a-q_b) \qquad (3)$$

$$+ 3 \sum_{q_a,q_b,q_c} (q_a.q)(2-q_a^2)A_{qa}A_{qb}A_{qc}\delta(q-q_a-q_b-q_c) \quad + \ldots.$$

where the wave numbers q and the time t have been nondimensionalized, using $1/q_M$ and $1/\sigma(q_M)$ as units of length (in the horizontal direction) and of time, and where the A_q are normalized by the initial thickness e_o. The presence of a second-order term in this equation is to be noted, and means that our system is not invariant by amplitude reflection. Usually in the physics of interfacial instabilities[10], this property tends to favor the occurence of an hexagonal symmetry. This tendency can be made more obvious by considering the growth of a pair of modes $\pm q_1$, with a perturbation of small amplitude on the two other pairs of modes $\pm q_2$ and $\pm q_3$ as suggested on figure (5).

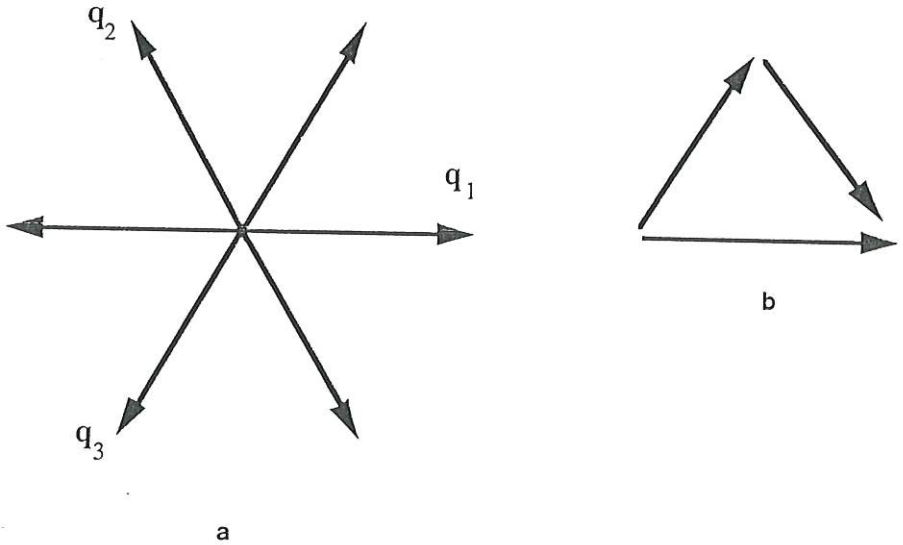

Fig. 5. (a) The three pairs of modes involved in our simplified discussion of the transition rolls-hexagons. (b) Selection rule associated to the second order non-linearity.

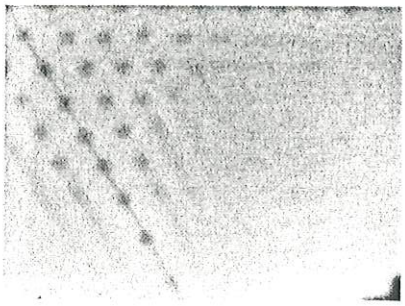

t = 360 s

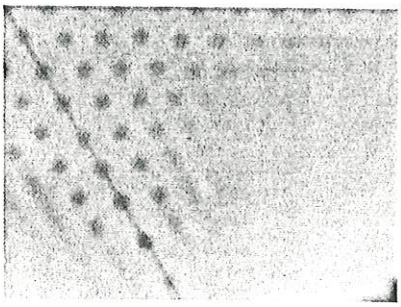

t = 480 s

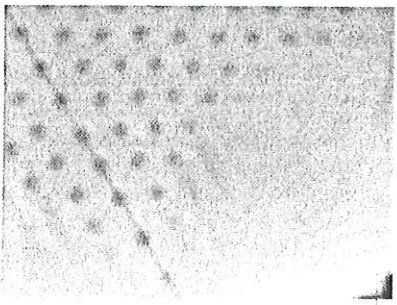

t = 600 s

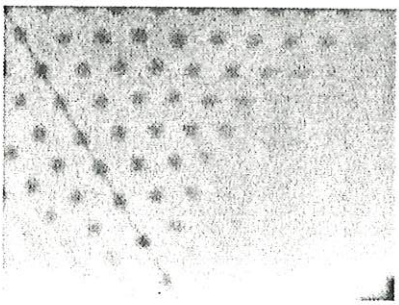

t = 720 s

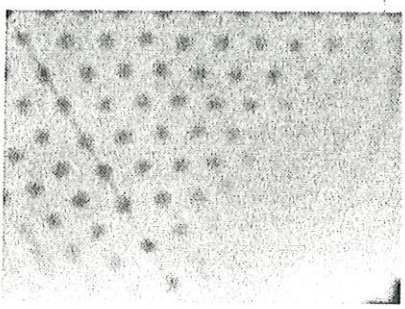

t = 840 s

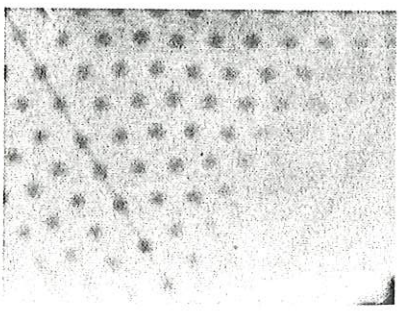

t = 960 s

Fig. 6. Time evolution of the instability initiated by two wires crossed at 60°.

This situation can also be understood as the competition between a roll pattern of amplitude $A_R(t)=A_{q1}-A_{q2}=A_{q1}-A_{q3}$ and an hexagonal pattern of small amplitude $A_H(t)=A_{q2}=A_{q3}$. For simplicity, the amplitudes are taken to be real, and only the most unstable wave-number $q_M=1$ is taken into account. At second order, eq. (3) reduces to:

$$\frac{dA_R}{dt} = A_R \qquad - 3\, A_R A_H$$

$$\frac{dA_H}{dt} = A_H + 3A_H^2 + 3A_H A_R \qquad (4)$$

In these equations, it is clear that the second order interaction suggested on figure (5 -b) tends to amplify the growth of the hexagonal perturbation, and to damp that of the roll pattern. We believe that this effect is the basic mechanism involved in the transition roll-hexagon .

ROLLS, SQUARE AND HEXAGONAL PATTERNS

The tendency of our system to develop a pattern with an hexagonal symmetry is enhanced if the initial perturbation is created by two wires crossed at 60° (fig. 6). As in the previous experiment two sets of "rolls" appear beside each wire. When the two sets of lines cross they create a perfect hexagonal pattern.

We have also try to force a pattern of square geometry by means of two wires crossed at 90°. The final result is presented on fig. (7) . The hexagonal symmetry is again clearly favored, but the square one seems to survive locally in some regions of the pancake. The "stability" (metastability is perhaps a better term) of this structure seems to be intermediate between that of the "rolls" and that of the hexagonal pattern.

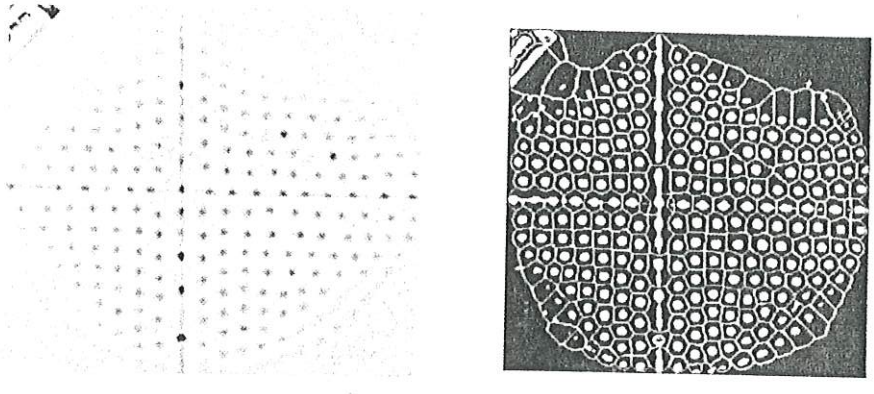

a b

Fig. 7. (a) final structure obtained with two wires crossed at 90°. (b) skeletonization obtained from image treatment. In some regions the square structure seems to survive.

A conclusion consistent with this observation can be obtained thoretically, by calculating the growth of the three patterns using a perturbation method, the initial amplitude ε being treated as a small parameter. At third order, this gives[1]:

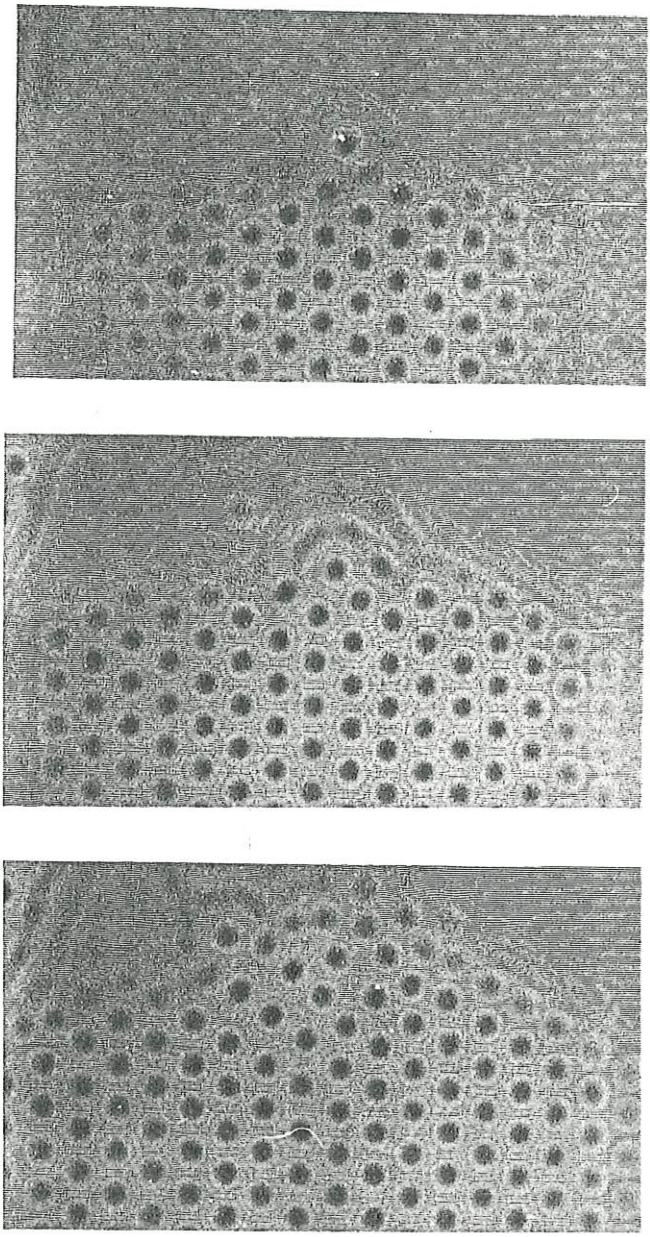

Fig. 8. Time evolution of a front between an hexagonal pattern and a region of unperturbed thickness. The hexagonal pattern has been forced by means of an array of needles. The deformation of the interface is revealed by observing a ruled screen across the oil layer. The time interval between pictures is 240 s.

$$A_R \approx \varepsilon e^t - 3\varepsilon^3 \left[e^{3t} - \frac{11}{8} e^t \right] + \ldots\ldots$$

$$A_S \approx \varepsilon e^t + \frac{9}{8}\varepsilon^3 e^t + \ldots \qquad (5)$$

$$A_H \approx \varepsilon e^t + 3\varepsilon^2 (e^{2t} - e^t) + \frac{1}{5}\varepsilon^3 \left[6e^{3t} - 96e^{2t} + \frac{1629}{8} e^t \right] + \ldots$$

where A_R, A_S and A_H are respectively the amplitudes of the "roll", square and hexagonal patterns.We see on these equations that the "rolls" are damped at third order, while the hexagonal pattern is amplified at second and third order. As announced above, the case of the square pattern is intermediate: at third order its growth is practically that obtained in the linear theory. It is also interesting to note that an hexagonal pattern of negative amplitude would be damped at second order. This means that an hexagonal lattice of "spikes" is amplified, while a lattice of "holes" would be damped. This situation results from the non-invariance by amplitude reflection of our system.

FRONT PROPAGATION PHENOMENA

Another typical feature of this instability appears on figs. (3,4,6). The patterns do not grow uniformly in space, but are in fact localized, their spatial extent increasing with time. This effect is particularly obvious on figure (6), where the "rolls" as well as the hexagonal systems exhibit a spreading dynamics. In analogy with what is observed in other instabilities[11], we suggest that this spreading may involve the propagation of a front[12-14] between a stable state (rolls or hexagons) and an unstable one (domain of unperturbed thickness). This idea can be precised by comparing the Swift Hohenberg model of convection

$$\frac{\partial u}{\partial t} = [\varepsilon - (1+\Delta)^2]u - u^3 \qquad (6)$$

to eq. (1) rewritten nondimensionally as:

$$\frac{\partial \zeta}{\partial t} = [1 - (1+\Delta)^2]\zeta - \nabla.[(3\zeta + 3\zeta^2 + \zeta^3)\nabla(2\zeta + \Delta\zeta)] \qquad (7)$$

As a first guess, we suggest that the front propagations in our experiment could be governed by the same linear mechanisms involved in the SH model (marginal stability case I), but with the control parameter ε being always equal to 1. This has allowed us to calculate the wave-length λ_L left behind the front, and the velocity of the front: $\lambda_L \approx 0.95\lambda_M$ and $v^* = 0.38 e_0^3 \rho^2 g^2 / \eta\gamma$ ($v^* = 4.6$ in adimensional units of eq. 7). The orders of magnitude obtained experimentally are consistent with this hypothesis. For instance, for the most regular patterns λ_L is of order 12.5 mm, that seems to be slightly smaller than our estimate for λ_M, $\lambda_M \approx 13.2$ mm , based on the value of γ given above. The theoretical value of v^* is difficult to determine because of its strong cubic dependance upon the layer thickness, that we did not measure accurately. The orders of magnitude $v^* \approx 0.05$ to 0.1mm/s are however consistent with the experiment. More accurate measurements, and a numerical study of front propagation in the case of equation (7) are under progress[15].

An interesting feature of our experiment is the possibility to observe two-dimensional aspects of front propagation. An example is given on figure (8), where a localized hexagonal pattern has been forced by means of an array of needles. At long time, it seems that the front parallel to one of the pair of wave-vectors is unstable and breaks in two fronts perpendicular to the two other pairs. The problem of two-dimensional front propagation has been scarcely studied, the only available study being that of Schiller[14]. We believe that our experiment could constitute an interesting tool of investigation of these problems.

The theoretical discussion of the development of instabilities in annular geometry is in general more difficult. We have developed in our case a simplified approach[1] based on the Fourier decomposition of the solutions of the linear problem. These solutions are of the kind:

$$\zeta_{q,n}(r,\theta,t) = J_n(qr)\cos(n\theta)\, e^{\sigma t} \qquad (8)$$

where J_n are the Bessel functions of the first kind, σ being again given by eq. (2). The Fourier content of these solutions corresponds to a continuous distribution of wave-vectors $\mathbf{q}$ of constant modulus q, which amplitude $a_n(\phi)=\cos(n\phi)$ depends on the azimuthal angle $\phi=(\mathbf{x},\mathbf{q})$. The same geometrical construction as that used for the hexagonal pattern (fig. 5-b) gives the second order coupling between the amplitudes $a_n(\phi,t)$ in a second order development[1]. After some calculations, one is led in this case to the conclusion that the patterns amplified at second order are of the kind:

$$\zeta = J_o(qr) + \alpha_1 J_6(qr)\cos(6\theta) + \alpha_2 J_{12}(qr)\cos(12\theta) + \ldots \qquad (9)$$

As mentioned more above, structures of this kind are very often nucleated by specks of dust falling on the interface. In their initial stage of evolution, only the J_0 component appears, while both the amplitude and the spatial extent of the pattern are growing. Later, a J_6 component may appear, very often by interference between two neighboring J_0 patterns. Qualitatively, this process is slower than the equivalent rolls-hexagons transition. We believe that the longer life-time of the axisymmetric pattern (J_0) is related to the fact that contrary to the "roll" pattern, it is amplified at second order. After the J_6 component, a J_{12} component appears, and so on. An example is given on fig. 9.

A careful analysis of the evolution of this kind of structure is under progress. We mention that sometimes, structures of five-fold or even seven-fold symmetry may also appear. An example is available on fig. 1.

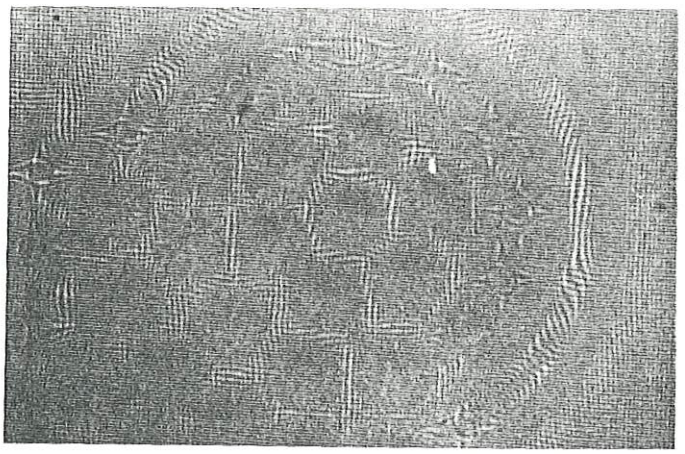

Fig. 9. Pattern obtained after transition of an axisymmetric structure towards the hexagonal symmetry. As in fig. 7, the thickness evolution is revealed by observing a ruled screen across the oil layer. Note the existence of 12 maximas on the second annulus, associated to the J_{12} component.

CONCLUSION

The Rayleigh-Taylor instability of a thin layer constitutes a nice example of a growth process driven by non-linearities. The observed behavior is very rich, involving a great variety of self organization phenomena: formation of two-dimensional patterns, transition between different symmetries, front propagation in two dimensions... The main mechanisms have been recognized, and more precise studies involving quantitative measurements, numerical simulations and theoretical calculations are now under progress.

Acknowledgment: we have benefitted from very helpful discussions with M. Brachet, H. Brand, G. Dewell, C. Mitescu, I. Mutabazi, J. C. Nataf, J. Prost, W. Van Saarloos and D. Walgraef. We also acknowledge helpful criticisms of the manuscript from R. Goodwin.

REFERENCES

1) M. Fermigier, L. Limat, J. E. Wesfreid, P. Boudinet and C. Quilliet, to appear in J. Fl. Mech.
2) M. Fermigier, L. Limat, J. E. Wesfreid, P. Boudinet, M. Petitjean, C. Quilliet and T. Valet, Phys. Fl. A 2, 1517 (1990).
3) S. Chandrasekhar, "Hydrodynamic and hydromagnetic stability", Dover (1981)
4) J. A. Whitehead and D. S. Luther, "J. Geophys. Res. 80, 705 (1975); J. A. Whitehead, Ann. Rev. Fl. Mech. 20, 61 (1988)
5) D. H. Sharp, Physica D 12, 3 (1984)
6) T. P. Hynes, "Stability of thin films", PHD Thesis, Cambridge Univ. (1978)
7) S. Yiantsios and B. G. Higgins, Phys. Fl. A 1, 1484 (1989).
8) J. Berenson, Int. J. Heat Mass Transfer, 5, 985 (1962)
9) J. Sainson, "Contribution à l'étude des transitions rapides de phase", Thesis, Université Paris 6 (1989); V. Hakim and J. Vannimenus, to be published.
10) E. Buzano and M. Golubitzky, Phil. Trans. Roy. Soc. (London) A 308, 617 (1983)
11) G. Ahlers and D. S. Cannell, Phys. Rev. Lett. 50, 1583 (1983)
12) G. Dee and J. S. Langer, Phys. Rev. Lett. 50, 383 (1983)
13) W. Van Saarloos Phys. Rev. A 37, 211 (1988); 39, 6367 (1989)
14) C. Schiller, "Modelisation of microstructures in metals", Thesis, Université Libre de Bruxelles (1989).
15) C. Mitescu, L. Limat and E. Wesfreid, Com. to 43rd APS Meeting, New-York (1990), Bull. Am. Soc. 35, 10, 2277 (1990).